

# Coulomb Oscillations at Room-Temperature of Single-Walled Carbon Nanotube Field-Effect Transistors

Y. Ohno\*, Y. Asai, K. Maehashi, K. Inoue and K. Matsumoto

\* The Institute of Scientific and Industrial Research, Osaka University  
8-1 Mihogaoka, Ibaraki, Osaka 567-0047, Japan, ohno@sanken.osaka-u.ac.jp

## ABSTRACT

Single-walled carbon nanotube field-effect transistors with thin tunnel barriers were fabricated, and room-temperature single-electron transistor operation was realized. Thin tunnel barrier layer, which was oxidized 1-nm-thick aluminum layer, was inserted between nanotube channel and electrodes in order to enhance carrier confinement. Gate voltage dependences of the drain current were measured at 290 K. Clear Coulomb oscillations could be observed for the sample with tunnel barrier layer while only conventional ambipolar characteristics of conventional carbon nanotube field-effect transistors could be observed for the sample without tunnel barrier layer. These results indicate that formation of thin tunnel barrier layer is very effective for realization of single-electron transistor operations at room temperature.

**Keywords:** carbon nanotube, field-effect transistors, single-electron transistors, Coulomb blockade, Coulomb oscillation

## 1 INTRODUCTION

Single-walled carbon nanotubes (SWNTs) are very attractive nano-meter-size materials for the building block of NEMS (Nano Electro Mechanical Systems) or quantum-effect based devices due to their extremely small diameter [1]. Among quantum-effect devices, single-electron transistors (SETs) are one of the most promising candidates for high-sensitive bio-molecule or single-spin sensors [2]. Broadly speaking, there are two kinds of SETs using carbon nanotube channels. One is the carbon nanotube field-effect transistor (CNT-FET) structures using tunnel barriers between SWNT channel and electrode [3]. In this case, SWNT channel is worked as a quantum dot. The other is the introducing some defects onto the SWNT channel surface by scanning-probe microscope or chemical process [2, 4, 5]. As these defect-introducing CNT-FETs have smaller quantum dot in the channel, they often showed SET behaviors at room temperature. Although they showed SET characteristics at room temperature, the fabrication process was rather complicated and reproducibility was not good. In this article, we focused the

tunnel barriers between SWNT channel and electrodes. Clear SET behaviors could be observed at low temperature (1.5 K) using these tunnel barrier, however, these SET behaviors disappeared above 160 K due to their small Coulomb charging energy of  $\sim 28$  meV, which is near thermal energy ( $k_B T$ ) at room temperature ( $\sim 26$  meV)[3]. Hence, we fabricated CNT-FETs with a thin  $\text{AlO}_x$  layer between SWNT channel and electrodes in order to enhance the carrier confinement.

## 2 EXPERIMENTAL

Figure 1 shows a schematic illustration of CNT-FETs used in this work. Using conventional photolithography, patterned 5-nm-thick cobalt layer which works as a chemical catalyst was deposited onto the Si/SiO<sub>2</sub> substrate by electron beam evaporator. Next, the substrate was put into the thermal chemical-vapor deposition (CVD) system and a quartz tube was exhausted by an oil-rotary pump until  $10^{-2}$  Torr, and the furnace was heated up to 820°C with flowing 1,000 sccm Ar gas. SWNTs were grown at 820°C and growth time was 10 min. Ethanol (C<sub>2</sub>H<sub>5</sub>OH) vapor was used as a carbon source. After growth of SWNTs, 1-nm-thick aluminum layer was deposited on SWNTs, and annealed at 350°C for 30 min in O<sub>2</sub> atmosphere in order to make  $\text{AlO}_x$  tunnel barrier layer. Then, Ti(1 nm)/Au(30 nm) source and drain electrodes were formed by photolithography and electron beam lithography. Finally, 10-nm-thick Au layer was deposited as a back gate electrode on the backside of the substrate. In this work, the distance between source and drain electrode was 300 nm. Current versus voltage characteristics were measured by the semiconductor device analyzer “Agilent B1500A” (Agilent Technologies, Inc.). Measurement temperature was changed by He gas cryostat from 7.5 K to room temperature.

## 3 RESULTS AND DISCUSSION

Drain current ( $I_D$ ) versus source-drain voltage ( $V_{SD}$ ) characteristics obtained from the CNT-FET with [with-out]  $\text{AlO}_x$  tunnel barrier were shown in Fig. 2(a) [Fig. 2(b)]. In this experiment, gate voltage ( $V_G$ ) was changed from -5 to 5 V with a 1 V step. In both CNT-FETs,  $I_D$  decreased at first with increasing  $V_G$  from -5 to 1 V, then, increased with more increasing  $V_G$ . These

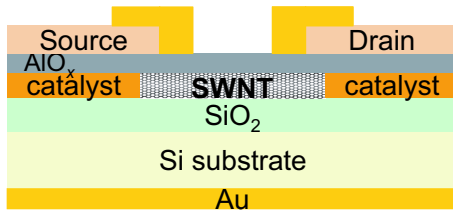


Figure 1: Schematic illustration of CNT-FETs with  $\text{AlO}_x$  tunnel barrier.

ambipolar  $I_D$ - $V_{SD}$  characteristics have been often observed from conventional CNT-FETs using semiconductor SWNT channel [6].

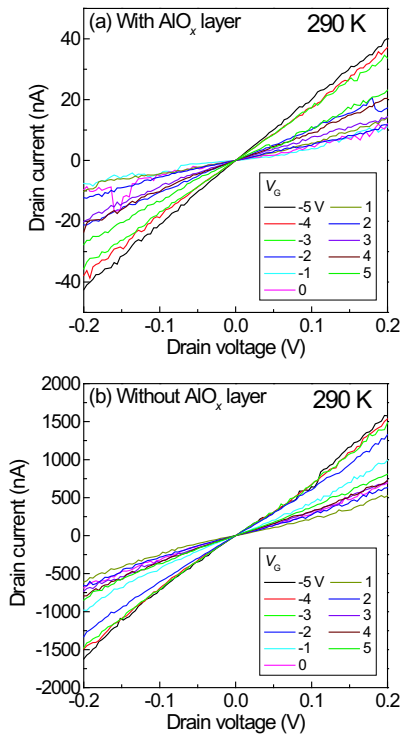


Figure 2:  $I_D$ - $V_{SD}$  characteristics of the CNT-FETs with (a) and without (b)  $\text{AlO}_x$  tunnel barrier layer.

The normalized  $I_D$ - $V_G$  characteristics ( $V_{SD} = 100$  mV) measured at 7.5, 150 and 290 K were shown in Fig. 3. Blue solid lines [red dashed lines] show the  $I_D$  of CNT-FETs with [without]  $\text{AlO}_x$  tunnel barrier layer. At 7.5 K, clear Coulomb oscillations could be seen for the both CNT-FETs. The average Coulomb oscillation interval ( $\Delta V_G$ ) was 0.37 and 0.35 V for the CNT-FET with and without  $\text{AlO}_x$  layer, respectively. These  $\Delta V_G$  corresponding to gate capacitance ( $C_G$ ) of 0.43 and

0.46 aF, which were derived from  $C_G = e/\Delta V_G$ . The Coulomb oscillations of the CNT-FETs without  $\text{AlO}_x$  layer gradually disappeared with increasing temperature, and conventional ambipolar CNT-FET characteristics could be seen at 290 K. In contrast, the clear Coulomb oscillations could be seen at even 290 K for the CNT-FET with  $\text{AlO}_x$  layer.

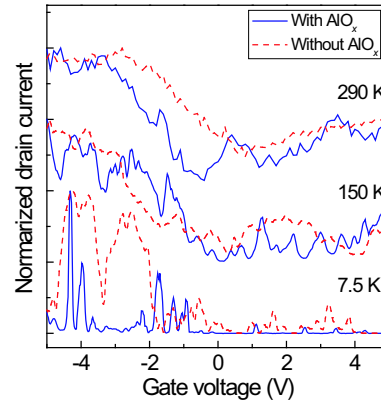


Figure 3: Temperature dependence of the normalized  $I_D$ - $V_G$  characteristics. The blue solid lines [red dashed lines] indicate the CNT-FET with [without]  $\text{AlO}_x$  tunnel barrier layer.

Figure 4 shows gray scale plots (contour plots) of the  $I_D$  as a function of both  $V_{SD}$  and  $V_G$  at 7.5 and 290 K. The results from the CNT-FET with [without]  $\text{AlO}_x$  layer were shown in Fig. 4(a) and Fig. 4(b) [Fig. 4(c) and Fig. 4(d)]. The black area indicates large value of the  $I_D$  and the white area shows smaller  $I_D$ . At 7.5 K, both of the CNT-FETs showed some diamond patterns. These diamond patterns is a well known as a consequence of Coulomb blockade, and the center of each cross is corresponding to a Coulomb blockade peak as shown in Fig. 3 [7]. Because of the degeneration of the ground state energies for  $n$  and  $n + 1$  carriers, current flows at this point. Therefore, no current flows in the diamonds. The maximum bias value ( $V_{Max}$ ) of the zero current region indicates the charging energy ( $E_C \sim eV_{Max}$ ). In our measurements, charging energy of CNT-FET with and without  $\text{AlO}_x$  layer for p-type FET region ( $-5 < V_G < -2$  V) was about 110 and 50 meV, respectively. The Coulomb diamonds of the CNT-FET without  $\text{AlO}_x$  layer disappeared at 290 K. Typical ambipolar gray scale plots for CNT-FETs could be seen. On the other hand, the Coulomb diamonds remained for the CNT-FET with  $\text{AlO}_x$  layer at 290 K, indicating the enhanced carrier confinement by the  $\text{AlO}_x$  tunnel barrier layer.

Here we applied very simple theoretical estimate [7]

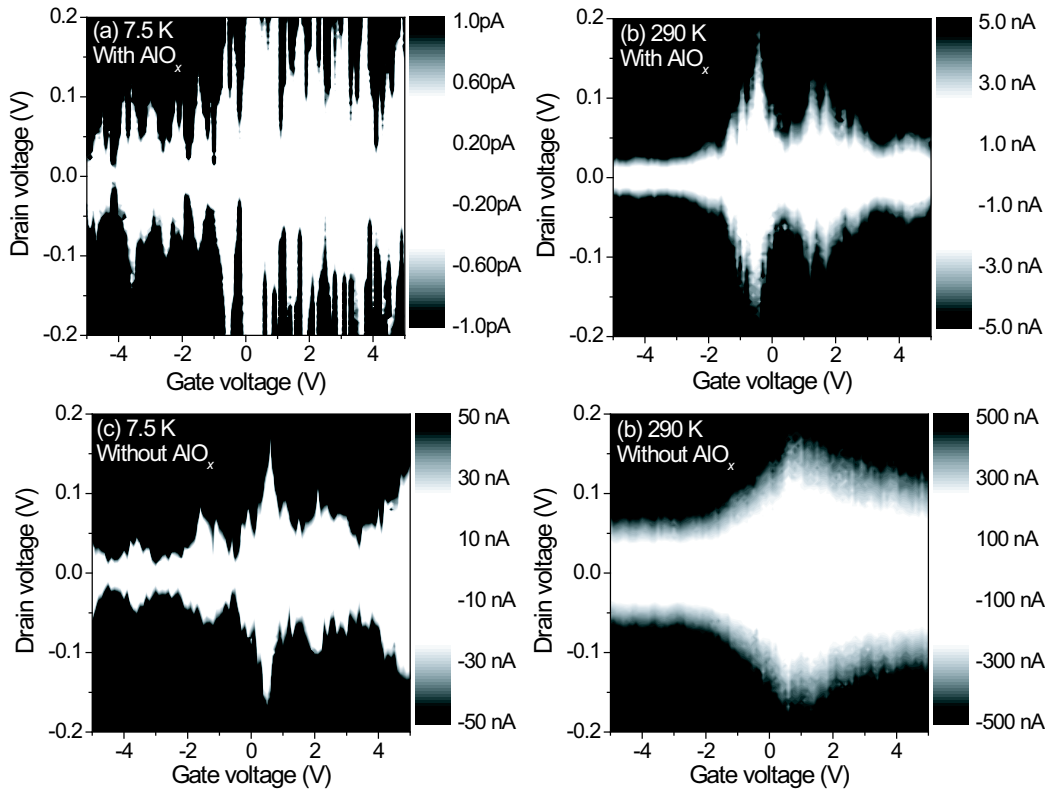


Figure 4: Gray scale plot of the  $I_D$  as a function of  $V_{SD}$  and  $V_G$  at 7.5 and 290 K.

for the length of SWNT quantum dot ( $L$ ) by

$$E_C = \frac{e^2}{C} \approx \frac{e^2}{\epsilon_r \epsilon_0 L} \approx \frac{5}{L [\mu\text{m}]} \text{ meV}, \quad (1)$$

where  $\epsilon_r = 4$  is the relative dielectric constant of appropriate for  $\text{SiO}_2$ . We obtain  $L \approx 45$  and  $100$  nm from the  $E_C$  for the CNT-FET with and without  $\text{AlO}_x$  layer, respectively. These  $L$  values were smaller than the lithographically defined contact separation for this CNT-FETs (the distance of the source and drain electrodes was  $300$  nm). It is noted that we neglect the exact sample configurations of electrodes, the surrounded SWNT channel by metallic pads makes the simple theoretical model difficult to apply to the actual CNT-FETs. From Fig. 3 and Fig. 4, some Coulomb oscillation peaks (Coulomb diamonds) of the CNT-FET with  $\text{AlO}_x$  layer were disappeared at  $290$  K, which indicate that some defects introduced onto the SWNT channel surface during growth or fabrication process. The simple theoretical model also agreed with this defect introduced SWNT channels. These defect-introduced SWNT channels have been known as a multi quantum dot structures [3], and it can be considered that the effective quantum dot

size is changed with increasing temperature.

We fabricated other CNT-FETs with the same fabrication process for confirmation of the reproducibility. As results,  $4/7$  of the CNT-FETs with  $\text{AlO}_x$  layer showed Coulomb oscillation at room temperature while  $1/6$  of the CNT-FETs without  $\text{AlO}_x$  layer showed Coulomb oscillation at room temperature. Obtained charging energies [the length of SWNT quantum dot from the eq. 1] were  $50 \sim 120$  meV [ $40 \sim 100$  nm] for CNT-FETs with  $\text{AlO}_x$  layer and  $50 \sim 90$  meV [ $55 \sim 100$  nm] for CNT-FETs without  $\text{AlO}_x$  layer. These results indicate that the realization of defect-free SWNT growth and fabrication process is very important for the CNT-FETs.

## 4 CONCLUSION

CNT-FETs with  $\text{AlO}_x$  layer as a tunnel barrier were investigated. Clear Coulomb oscillations could be observed at  $290$  K from the CNT-FET with  $\text{AlO}_x$  layer while typical ambipolar characteristics observed for the CNT-FET without  $\text{AlO}_x$  layer. It can be considered that the carrier confinement enhanced by the  $\text{AlO}_x$  layer. These results indicate that formation of thin tun-

nel barrier layer between SWNT channel and electrode pads is very effective for realization of SET operations at room temperature. We will apply the SETs for high-sensitive bio-molecule sensors in the future.

## ACKNOWLEDGEMENTS

This research was partially supported by Core Research for Evolutional Science and Technology (CREST), the Japan Science and Technology Corporation (JST), the New Energy and Industrial Technology Development Organization (NEDO), and “Special Coordination Funds for Promoting Science and Technology: Yuragi Project” of the Ministry of Education, Culture, Sports, Science and Technology, Japan. One of the authors (K. I.) was supported in part by a Grant-in-Aid for Scientific Research from the Japan Society for the Promotion of Science.

## REFERENCES

- [1] S. Iijima and T. Ichihashi, *Nature* 363, 603, 1993.
- [2] K. Matsumoto, S. Kinoshita, Y. Gotoh, K. Kurachi, T. Kamimura, M. Maeda, K. Sakamoto, M. Kuwahara, N. Atoda and Y. Awano, *Jpn. J. Appl. Phys.* 42, 2415, 2003.
- [3] D. Tsuya, M. Suzuki, Y. Aoyagi and K. Ishibashi, *Jpn. J. Appl. Phys.* 44, 2596, 2005.
- [4] C. K. Hyon, A. Kojima, T. Kamimura, M. Maeda and K. Matsumoto, *Jpn. J. Appl. Phys.* 44, 2056, (2005).
- [5] K. Maehashi, H. Ozaki, Y. Ohno, K. Inoue, K. Matsumoto, S. Seki and S. Tagawa, *Appl. Phys. Lett.* 90, 023103, 2007.
- [6] T. Mizutani, S. Iwatsuki, Y. Ohno and S. Kishimoto, *Jpn. J. Appl. Phys.* 44, 1599, 2005.
- [7] J. Nygard, D. H. Cobden, M. Bockrath, P. L. McEuen and P. E. Lindelof, *Appl. Phys. A* 69, 297, 1999.